

## LABORATORY H<sub>2</sub>O:CO<sub>2</sub> ICE DESORPTION: ENTRAPMENT AND ITS PARAMETERIZATION WITH AN EXTENDED THREE-PHASE MODEL

E.C. Fayolle<sup>1</sup>, K.I. Öberg<sup>2</sup>, H.M. Cuppen<sup>3</sup>, R. Visser<sup>4</sup> and H. Linnartz<sup>1</sup>

**Abstract.** Ice desorption affects the evolution of the gas-phase chemistry during the protostellar stage, and also determines the ice composition of comets forming in circumstellar disks. From observations, most volatile species, including CO<sub>2</sub>, are found in H<sub>2</sub>O-dominated ices. In this study, the desorption of CO<sub>2</sub> mixed in H<sub>2</sub>O ice and the impact of ice thickness, mixture ratio and heating rate are experimentally determined. The results are used to parametrize an extended three-phase model (gas, ice surface and ice mantle) which describes ice mixture desorption using rate equations and a minimum number of free parameters. The model can be used to predict the evolution in thickness and concentration of volatile-rich H<sub>2</sub>O ice during infall of icy grains around protostars.

### 1 Astrophysical context

In pre-stellar cores, cold outer protostellar envelopes and protoplanetary disk mid-planes, most molecules, except for H<sub>2</sub>, are frozen out on dust grains, forming ice mantles. The main ice component around young stellar objects is H<sub>2</sub>O, followed in abundance by CO and CO<sub>2</sub> according to Spitzer observations (Öberg *et al.* 2011). Infrared observations of pre-stellar cores show that most CO<sub>2</sub> ice and some of the CO ice is mixed with H<sub>2</sub>O (Knez *et al.* 2005). Based on these observations, H<sub>2</sub>O and CO<sub>2</sub> are thought to form simultaneously on the grain surface during the early stage of cloud formation (Pontoppidan *et al.* 2008). Once the protostar is formed,

---

<sup>1</sup> Sackler Laboratory for Astrophysics, Leiden Observatory, Leiden University, PO Box 9513, 2300 RA Leiden, The Netherlands

<sup>2</sup> Harvard-Smithsonian Center for Astrophysics, MS 42, 60 Garden Street, Cambridge, MA 02138, USA

<sup>3</sup> Institute for Molecules and Materials, Radboud University Nijmegen, PO Box 9010, 6500 GL Nijmegen, The Netherlands

<sup>4</sup> Department of Astronomy, University of Michigan, 500 Church Street, Ann Arbor, MI 48109-1042, USA

it heats its environment, including the icy grains. This results in the desorption of the water-rich layer (Pontoppidan *et al.* 2008). The ice desorption impacts on the amount of molecules available for chemical reactions in both gas and solid phase. It is therefore crucial to understand water-rich ice desorption and to implement it effectively in astrochemical networks.

Laboratory experiments have shown that ice mixture desorption is not as straight forward as pure ice desorption. A wide variety of interactions between H<sub>2</sub>O molecules and volatile species is responsible for the trapping of volatiles in the water ice. Volatile components therefore desorb from H<sub>2</sub>O-rich ice mixtures at a minimum of two different temperatures, corresponding to the desorption of the species from the surface of the H<sub>2</sub>O ice and from molecules trapped inside the bulk of the H<sub>2</sub>O ice that only start desorbing at the onset of H<sub>2</sub>O desorption. The fraction of trapped volatiles may vary with ice characteristics such as thickness, concentration and heating rate. This is investigated here and used to parameterize a model that can simulate ice mixture desorption around protostars.

Details of this work are available from Fayolle *et al.* (2011).

## 2 Ice mixture desorption experiments

The experiments in this study are chosen simultaneously to provide data directly relevant to ice desorption in different astrophysical environments (with different ices) and to construct a proof-of-concept model for ice mixture desorption. All desorption experiments are performed with CRYOPAD. This set-up has been described in detail by Fuchs *et al.* (2006). The set-up consists of an ultra high vacuum (UHV) chamber with a base pressure of  $\sim 10^{-10}$  mbar at room temperature. Ices are grown on a gold-coated substrate situated at the center of the chamber that can be cooled down to 16 K. Fourier Transform Reflection Absorption Infrared Spectroscopy (FT-RAIRS) is used to monitor molecules condensed on the gold surface. Ice evaporation is induced by linear heating of the substrate (and ice) in temperature programmed desorption (TPD) experiments. A quadrupole mass spectrometer (QMS) continuously analyzes the gas-phase composition mass-selectively with the goal to record desorption curves of evaporating molecules during the TPD experiments. The H<sub>2</sub>O and CO<sub>2</sub> ice amounts are determined directly using RAIRS.

Figure 1 shows the output of typical desorption experiments. In the upper panel, an H<sub>2</sub>O:CO<sub>2</sub> ice mixture is slowly heated at 1K/min from 20 to 160 K. The mass spectrometer monitors at the same time the desorbing CO<sub>2</sub>. Carbon dioxide desorbs at two distinct temperatures: its own desorption temperature (first peak at 75 K), and at a higher temperature when the H<sub>2</sub>O is also desorbing. The lower panel of Figure 1 presents the desorption of pure CO<sub>2</sub> and H<sub>2</sub>O for comparison. Such experiments allow for quantification of the amount of CO<sub>2</sub> that stays trapped in the H<sub>2</sub>O ice (peak at higher temperature). By integrating the second peak over the entire desorption plot, a trapping fraction is derived. Experiments for various H<sub>2</sub>O:CO<sub>2</sub> ice ratios, thicknesses and heating rates were performed to constrain the influence of the ice properties on the trapping efficiency.

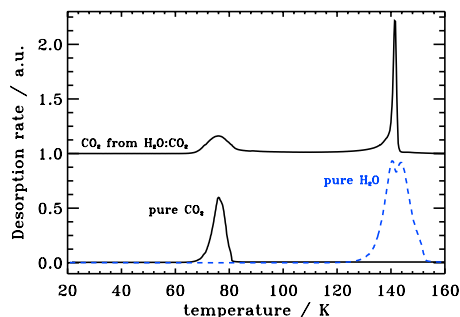


**Fig. 1.** The upper panel presents the signal of gas phase CO<sub>2</sub> detected by the QMS while a H<sub>2</sub>O:CO<sub>2</sub> 5:1 ice of 18 ML is linearly heated at 1K/min. The lower panel presents the desorbing signal of pure CO<sub>2</sub> ice (solid line) and pure H<sub>2</sub>O ice (dashed line). This illustrates that when in water mixture, CO<sub>2</sub> desorbs at both its own desorption temperature (first peak at 75 K), and at higher ice temperature when the H<sub>2</sub>O is also desorbing.

H<sub>2</sub>O:CO<sub>2</sub> ice thicknesses over the 10–32 ML range were investigated and it was found that the amount of trapped CO<sub>2</sub> increases with ice thickness. In contrast, the amount of CO<sub>2</sub> desorbing around 75 K is independent of ice thickness. This implies that only CO<sub>2</sub> molecules from the top part of the ice are available for desorption at the CO<sub>2</sub> desorption temperature. This can be explained by either a highly porous ice that allows CO<sub>2</sub> to freely desorb from the top layers or by diffusion from the top layers of the mantle phase to the surface. In both cases the surface is eventually totally saturated by water molecules, trapping the rest of the volatiles in the ice mantle.

When increasing the concentration of CO<sub>2</sub> in H<sub>2</sub>O ice, the trapped fraction decreases; the number of pores exposed to the surface or the diffusion length scale of volatiles in the ice must increase with increasing volatile concentration. Increased diffusion may either be due to a gradually looser binding environment in the volatile-rich ices or a break-down of H<sub>2</sub>O ice structure in the presence of higher concentrations of volatiles.

TPD experiments were performed at different heating rates, from 0.5 to 5 K/min, but this parameter does not appreciably affect the trapping efficiency of CO<sub>2</sub> in the H<sub>2</sub>O ice. This implies that there is a rather sharp boundary between the molecules in the upper layers that can diffuse to the surface (whether through pores or bulk diffusion) and molecules deeper in the ice that cannot. Even if the volatiles deep in the ice can diffuse within the ice mantle, diffusion upwards must quickly become slow as the surface layers saturate with H<sub>2</sub>O molecules or alternatively all accessible pores have been emptied.

### 3 Desorption and three-phase model – Gas, ice surface and bulk

The model used here to simulate the trapping of volatile species in a water dominated ice is based on the three-phase model of Hasegawa & Herbst (1993). In

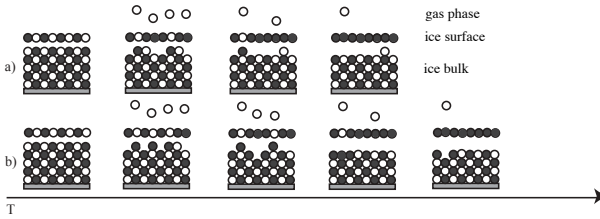


**Fig. 2.** A cartoon of desorption within the three-phase model of a binary mixture with a volatile component (white) and  $\text{H}_2\text{O}$  (black), before the onset of  $\text{H}_2\text{O}$  desorption. Only surface molecules can desorb. In the original three-phase model (a) the surface is replenished statistically according to mantle composition alone (Hasegawa & Herbst 1993). In the extended model of Fayolle *et al.* (2011) (b) the mantle-to-surface diffusion accounts for ice segregation of volatile species to the surface, reducing the amount of trapped volatile species.

this model, gas-grain interactions are addressed by considering three phases: the gas phase, the surface of the ice and the bulk/mantle of the ice. When looking at the thermal desorption only, the model is based on the principle that molecules can only desorb from the surface into the gas phase, using a zeroth-order Polanyi-Wigner equation, and that the mantle molecules migrate to the surface following the desorption of a surface molecule statistically. In the Hasegawa & Herbst (1993) model, this mantle to surface migration depends only on the mixing ratio of each species, *e.g.*, for a  $\text{H}_2\text{O}:\text{CO}_2$  1:1 ice mixture, a molecule that desorbs into the gas phase has a 50% chance of being replaced by a water molecule and a 50% chance of being replaced by a  $\text{CO}_2$  molecule, as depicted in panel a) of Figure 2.

This migration mechanism does not account for the preferred replenishment of the surface phase by volatile mantle species or that volatile species may diffuse more easily in the ice compared to water. Segregation observed both in the laboratory (Öberg *et al.* 2009) and in space (Pontoppidan *et al.* 2008) clearly shows the importance of diffusion. Our proposed extension of the three-phase model accounts for this by introducing a mantle-surface diffusion term. Trapping of volatiles still occurs but the surface-mantle diffusion of volatiles is enhanced compared to the original model. This diffusion term physically includes two free parameters: the energy barrier that a volatile molecule has to overcome to swap with a neighboring  $\text{H}_2\text{O}$  molecule and the fraction of mantle molecules close enough to participate in the swapping with surface molecules. A mathematical description of these parameters is available from Fayolle *et al.* (2011) and values are found using the  $\text{H}_2\text{O}:\text{CO}_2$  experiments described in the previous section. A chi-squared fit of the model trapping fraction compared to the experimental trapping fraction returned the two free parameter best values and experimental trapping efficiency trends with thickness, mixing ratio and heating rate, are reproduced. The predictive power of the model has been tested on  $\text{H}_2\text{O}:\text{CO}_2:\text{CO}$  mixtures and results in trapping efficiencies in good agreement with experiment.

## 4 Consequences for astrochemical networks

When running simulations at 1 K per century, typical for an infall rate during protostar formation, the model shows that the trapping efficiency is highly affected by the initial ice thickness and the mixing ratio. For example, a 5:1 H<sub>2</sub>O:CO<sub>2</sub> mixture of 10 ML will result in 50% entrapment but the same mixture 100 ML thick will see 95% of its CO<sub>2</sub> content trapped within the water matrix. This shows that it is vital to understand how ice mixture desorption depends on the ice characteristics and to consider entrapment of volatiles in water ice when including desorption in astrochemical networks.

## References

- Fayolle, E.C., Öberg, K.I., Cuppen, H.M., Visser, R., & Linnartz, H., 2011, *A&A*, 529, A74
- Fuchs, G.W., Acharyya, K., Bisschop, S.E., Öberg, *et al.*, 2006, *Faraday Discuss.*, 133, 331
- Hasegawa, T.I., & Herbst, E., 1993, *MNRAS*, 263, 589
- Knez, C., Boogert, A.C.A., Pontoppidan, K.M., Kessler-Silacci, *et al.*, 2005, *ApJ*, 635, L145
- Öberg, K.I., Boogert, A.C.A., Pontoppidan, K.M., *et al.*, 2011, *ApJ*, 740, 109
- Öberg, K.I., Fayolle, E.C., Cuppen, H.M., van Dishoeck, E.F., & Linnartz, H., 2009, *A&A*, 505, 183
- Pontoppidan, K.M., Boogert, A.C.A., Fraser, H.J., *et al.*, 2008, *ApJ*, 678, 1005